ISBN: 978-3-95450-262-2 ISSN: 2673-5350 doi: 10.18429/JACoW-IBIC2025-WEPCO20

# DEVELOPMENT OF NOVEL, RADIATION-HARD, ULTRA-COMPACT ACTIVE BEAMSTOPS WITH INTEGRATED 4-QUADRANT X-RAY SENSORS FOR SCATTERING EXPERIMENTS ON HIGH-BRILLIANCE UNDULATOR BEAMLINES

G. Trovato[1,2,3,4], K. Nygard[5], M. Birri[6], D. F. Sanchez[6],
D. Grolimund[6], N. La Rosa[2,7], S. Moscato[2,7], M. Camarda[2,3,7]
[1]Dipartimento di Fisica e Astronomia "E. Majorana", Università degli studi di Catania, Catania, Italy
[2]STLab s.r.l., Catania, Italy
[3]CNR-IMM, Catania, Italy
[4]Istituto Nazionale di Fisica Nucleare, Sezione di Catania, Catania, Italy
[5]MAX IV Laboratory, Lund University, Lund, Sweden
[6]Swiss Light Source, Paul Scherrer Institute, Villigen, Switzerland
[7]DIEEI, Via Santa Sofia, Catania Italy
[8]SenSiC GmbH, Villigen, Switzerland

## ABSTRACT

Beamstopper-Integrated Sensors (BIS) based on silicon carbide (SiC) represent a novel class of compact, radiation hard devices that combine beam interception with real-time diagnostics. We present the first characterization of four-quadrant BIS designed for simultaneous intensity and position monitoring on synchrotron beamlines. Based on the established reliability of single-pixel BIS as intensity monitors at SLS, we demonstrate quadrant-resolved response and linearity with photon flux, despite minor contacting issues in one channel. These results establish SiC BIS as robust, visible-blind diagnostics, leading the way for deployment of position-sensitive BIS in high-brilliance undulator experiments.

## INTRODUCTION

Previous generations of so-called 'active beamstops' attempted to integrate sensing functionality by embedding silicon diodes either directly exposed to the beam [1] or indirectly detecting backscattered photons [2]. Although these pioneering devices provided the first proof-of-concept of beamstop-integrated diagnostics, they were limited by radiation damage, energy-dependent sensitivity, and challenges in miniaturization. The Beamstopper-Integrated Sensor (BIS) represents a new approach, based on silicon carbide (SiC) as the sensing material (Fig. 1). SiC offers a wide bandgap, intrinsic insensitivity to visible light, high thermal conductivity, and extraordinary radiation hardness [3], enabling stable long-term operation even under the most intense synchrotron and XFEL beams. These properties allow BIS devices to provide both intensity monitoring and beam position sensing in ultra-compact footprints (<1 mm), while maintaining robustness and reliability. SiC-based BIS are no longer at the prototype stage: they have been extensively deployed as intensity monitors ($I_0$) at the microXAS beamline of the Swiss Light Source (SLS-PSI), where they have been permanently used for several years across a broad spectrum of scientific experiments.

Figure 1: Left) BiS as intensity monitor, packaging. Right) BiS in operation.

Publications using SiC BIS as flux monitors include environmental and life science applications, such as studies of cyanobacterial microfossils [4], arsenic detoxification in microbial mats [5], and toxicokinetics of uranium nanoparticles in aquatic organisms [6–8]. In parallel, SiC BIS have supported biomedical and materials research, including bone fracture healing [9], zirconium hydride phase mapping in Zircaloy-2 [10], and electrochemical studies of solid oxide cell electrodes and coatings [11, 12]. In the field of additive manufacturing, BIS-enabled operando X-ray diffraction and scattering experiments have been reported in studies of titanium alloys [13–15], steels [16], and programmable alloys [17]. Furthermore, BIS have been instrumental in energy research, including operando studies of Li–air batteries [18]. These results on BIS for intensity monitoring demonstrate that the sensors are reliable and radiation hard, providing robust support for scattering experiments on high-brilliance undulator beamlines. Based on this extensive validation, we now present the first dedicated characterization of BIS devices as position sensors, with the goal of extending their functionalities and enabling novel experiments that exploit post-sample beam position information as an additional diagnostic, complementing the measurements already available.

ISBN: 978-3-95450-262-2 ISSN: 2673-5350 doi: 10.18429/JACoW-IBIC2025-WEPCO20



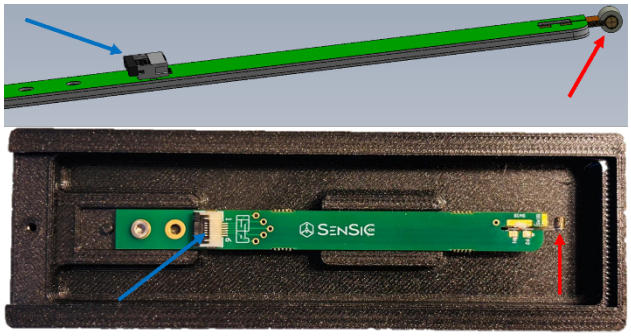


Figure 2: Top) Schematic of a BIS with absorber, SiC sensor, and readout interface. Bottom) Photo of the prototype.

## MATERIALS AND METHODS

General BIS devices (Fig. 2) consist of a SiC sensing layer bonded to a heavy metal absorber (Ag or W), ensuring complete beam absorption while allowing current readout. The device footprints currently range from 2 mm to 3 mm in diameter with four separate quadrants (position) for position sensitivity.

Similarly to the intensity monitor, each BIS is mounted on a thin PCB with encapsulated electrical contact, providing robust external connections through flat cables and LEMO contacts. Wirebond-free glue bonding ensures mechanical robustness and easy handling. Installation procedure is simplified by simple tests using UV sources, exploiting the visible light blindness of SiC.

## RESULTS AND CONCLUSIONS

Figure 3 shows the spatial response of a four-quadrant BIS obtained using a 2D beam scan. Each quadrant delivers a distinct and localized signal, demonstrating the capability of the device to resolve beam position after the sample. Channels 1, 2, and 4 exhibit stable signals across the scanned region, with sharp transitions at the quadrant boundaries, confirming the proper segmentation of the sensing area.

Channel 3, in this configuration, remained inactive due to a contacting issue during assembly, highlighting an area of technical optimization that is currently under investigation. In addition, the linearity of the quadrant signals with respect to the incident photon flux was verified (Fig. 4). Channels 1, 2, and 4 show highly linear responses with average currents of 30.8 µA, 27.9 µA, and 20.3 µA respectively, and standard deviations below 1 µA across the tested flux range. These results confirm the excellent reproducibility and reliability of the SiC sensor response, in line with previous observations for single-pixel intensity BIS.

The results presented here extend the validation of silicon carbide Beamstopper-Integrated Sensors (BIS) from intensity monitoring to position-sensitive operation. The quadrant devices demonstrate robust spatial discrimination and linearity with photon flux, essential for precision diagnostics in scattering experiments on high-brilliance undulator beamlines. Thanks to the already well established track record of intensity mode BIS as reliable and radiation-hard monitors, and once the contacting issue affecting one quadrant is resolved, the four-quadrant BIS will be ready for deployment as standard diagnostic tools in synchrotron and FEL facilities.

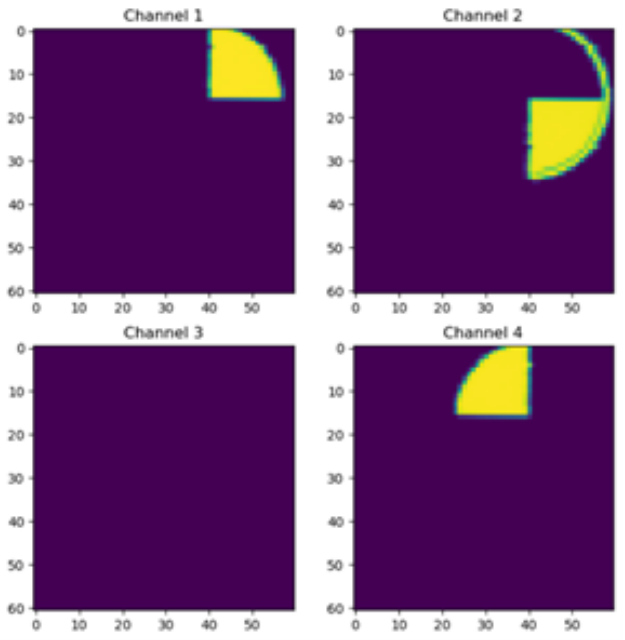


Figure 3: 2D beam scan of the 4-quadrant BIS using a 50 µA x 50 µA beam, $1 \times 10^{13}$ ph/s with energy of 16.5 keV.

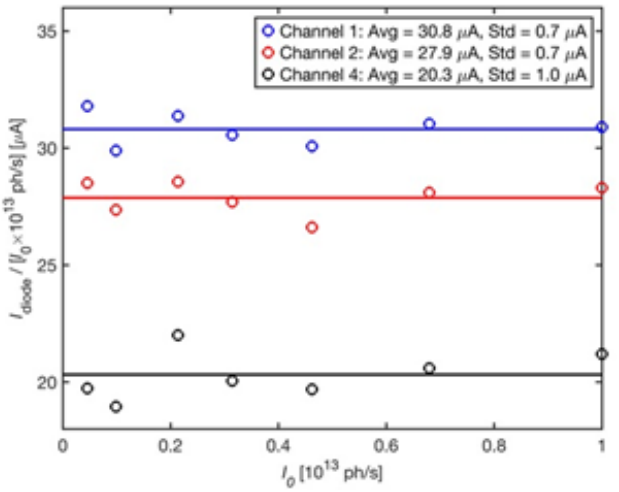


Figure 4: Linearity of the quadrant signals with respect to the incident photon flux.

## REFERENCES

[1] P. J. Ellis, A. E. Cohen, and S. M. Soltis, "Beamstop with integrated X-ray sensor", *J. Synchrotron Radiat.*, vol. 10, pp. 287–288, 2003. doi:10.1107/S0909049503003285

[2] C. E. Blanchet, C. Hermes, D. I. Svergun, and S. Fiedler, "A small and robust active beamstop for scattering experiments on high-brilliance undulator beamlines", *J. Synchrotron Radiat.*, vol. 22, no. 2, pp. 461–464, 2015. doi:10.1107/S160057751402829X

ISBN: 978-3-95450-262-2 ISSN: 2673-5350 doi: 10.18429/JACoW-IBIC2025-WEPCO20

[3] M. De Napoli, "SiC detectors: A review on the use of silicon carbide as radiation detection material", *Front. Phys.*, vol. 10, p. 898833, 2022. doi:10.3389/fphy.2022.898833

[4] C. F. Demoulin *et al.*, "Polysphaeroides filiformis, a proterozoic cyanobacterial microfossil and implications for cyanobacteria evolution", *iScience*, vol. 27, no. 2, p. 108865, 2024. doi:10.1016/j.isci.2024.108865

[5] C. Thomas *et al.*, "Combined genomic and imaging techniques show intense arsenic enrichment caused by detoxification in a microbial mat of the Dead Sea shore", *Geochem. Geophys. Geosyst.*, vol. 25, no. 3, p. 2023GC011239, 2024. doi:10.1029/2023GC011239

[6] I. Byrnes *et al.*, "Synchrotron-based X-ray fluorescence imaging elucidates uranium toxicokinetics in *Daphnia magna*", *ACS Nano*, vol. 17, no. 6, pp. 5296–5305, 2023. doi:10.1021/acsnano.2c06111

[7] I. Byrnes *et al.*, "Synchrotron XRF and histological analyses identify damage to digestive tract of uranium NP-exposed *Daphnia magna*", *Environ. Sci. Technol.*, vol. 57, no. 2, pp. 1071–1079, 2023. doi:10.1021/acs.est.2c07174

[8] C. M. Fallon *et al.*, "Vadose-zone alteration of metaschoepite and ceramic $UO_2$ in Savannah River Site field lysimeters", *Sci. Total Environ.*, vol. 862, p. 160862, 2023. doi:10.1016/j.scitotenv.2022.160862

[9] H. Dejea *et al.*, "Multi-scale characterization of the spatiotemporal interplay between elemental composition, mineral deposition and remodelling in bone fracture healing", *Acta Biomater.*, vol. 167, pp. 135–146, 2023. doi:10.1016/j.actbio.2023.06.031

[10] A. W. Colldeweih, M. G. Makowska, O. Tabai, D. F. Sanchez, and J. Bertsch, "Zirconium hydride phase mapping in Zircaloy-2 cladding after delayed hydride cracking", *Materialia*, vol. 27, p. 101689, 2023. doi:10.1016/j.mtla.2023.101689

[11] L. Yefsah *et al.*, "Electrochemical performance and stability of $PrO_{1.833}$ as an oxygen electrode for solid oxide electrolysis cells", *Solid State Ionics*, vol. 399, p. 116316, 2023. doi:10.1016/j.ssi.2023.116316

[12] J. Ignaczak *et al.*, "Fe-modified $Mn_2CuO_4$ spinel oxides: coatings based on abundant elements for solid oxide cell interconnects", *Int. J. Hydrogen Energy*, vol. 48, no. 27, pp. 36076–36093, 2023. doi:10.1016/j.ijhydene.2023.06.041

[13] M. Chen *et al.*, "A quantitative study of thermal cycling along the build direction of Ti-6Al-4V produced by laser powder bed fusion", *Mater. Des.*, vol. 225, p. 111458, 2023. doi:10.1016/j.matdes.2022.111458

[14] R. Esmaeilzadeh *et al.*, "In-situ selective laser heat treatment for microstructural control of additively manufactured Ti-6Al-4V", *Addit. Manuf.*, vol. 78, p. 103882, 2023. doi:10.1016/j.addma.2023.103882

[15] P. Scheel *et al.*, "A close look at temperature profiles during laser powder bed fusion using operando X-ray diffraction and finite element simulations", *Addit. Manuf. Lett.*, vol. 6, p. 100150, 2023. doi:10.1016/j.addlet.2023.100150

[16] H. H. König *et al.*, "Solidification modes during additive manufacturing of steel revealed by high-speed X-ray diffraction", *Acta Mater.*, vol. 246, p. 118713, 2023. doi:10.1016/j.actamat.2023.118713

[17] S. Gao *et al.*, "Additive manufacturing of alloys with programmable microstructure and properties", *Nat. Commun.*, vol. 14, p. 6752, 2023. doi:10.1038/s41467-023-42326-y

[18] C. G. Anchieta *et al.*, "LiOH decomposition by $NiO/ZrO_2$ in Li–air batteries: chemical imaging with operando synchrotron diffraction and correlative neutron/X-ray computed tomography analysis", *Small Methods*, vol. 8, no. 10, p. 2301749, 2024. doi:10.1002/smtd.202301749